

Contents lists available at [SciVerse ScienceDirect](#)

# Bioorganic & Medicinal Chemistry Letters

journal homepage: [www.elsevier.com/locate/bmcl](http://www.elsevier.com/locate/bmcl)

## Hydantoin based inhibitors of MMP13—Discovery of AZD6605



Chris De Savi<sup>a,b,\*</sup>, David Waterson<sup>b</sup>, Andrew Pape<sup>b</sup>, Scott Lamont<sup>b</sup>, Elma Hadley<sup>b</sup>, Mark Mills<sup>b</sup>, Ken M. Page<sup>b</sup>, Jonathan Bowyer<sup>b</sup>, Rose A. Maciewicz<sup>b</sup>

<sup>a</sup> Oncology Innovative Medicines, AstraZeneca R&D Boston, 35 Gatehouse Drive, Waltham, MA 02451, United States

<sup>b</sup> Respiratory and Inflammation Innovative Medicines, AstraZeneca R&D Molndal, SE-43813 Molndal, Sweden

### ARTICLE INFO

#### Article history:

Received 7 April 2013

Revised 24 May 2013

Accepted 28 May 2013

Available online 10 June 2013

#### Keywords:

MMP13

Hydantoin

Zinc binder

Cyp P450

Lead optimisation

### ABSTRACT

Piperidine ether and aryl piperazine hydantoins are reported as potent inhibitors of MMP13. A medicinal chemistry campaign focused on replacing the reverse hydroxamate zinc binding group associated with historical inhibitors with a hydantoin zinc binding group then optimising MMP13 potency, solubility and DMPK properties whilst maintaining good selectivity over MMP14. A number of high quality candidates were progressed and following rat and dog safety evaluation, AZD6605 (**3m**) was identified as a candidate drug.

© 2013 Elsevier Ltd. All rights reserved.

Osteoarthritis (OA) is a heterogeneous group of conditions sharing common pathologic and radiologic features.<sup>1</sup> OA is a non-overtly inflammatory degenerative joint disease with a wide range of presentations, from asymptomatic to seriously disabling. It is extremely common and age-related and is often accompanied by clinical manifestations such as use-related joint pain and loss of joint movement. OA is one of the last remaining poorly treated chronic conditions, which has huge health economic impacts.<sup>2,3</sup> The only treatments are pain relief (e.g., NSAIDs and COX-II)<sup>4</sup> and surgery.

The activity of matrix metalloproteinases (MMPs), a family of 24 zinc-dependent neutral endopeptidases, has been implicated in both physiological and pathological tissue remodelling,<sup>5</sup> as they are collectively capable of degrading essentially all of the components of the extracellular matrix. One of the MMPs, MMP13, also known as Collagenase 3, is thought to have a major role in degrading type II collagen,<sup>6</sup> which provides cartilage with its structural integrity. In adults, MMP13 is expressed only in pathological tissue. Matrix metalloproteinase inhibitors (MMPi's) have been studied for many years as possible drugs for prevention of cartilage degradation but their clinical use has been hampered by severe musculoskeletal side effects commonly characterized by joint stiffness and pain.<sup>7,8</sup> It is still not known which metalloproteinases contribute to the fibrodysplasia but it is likely to be due to the combined inhibition of a combination of several critical MMPs such as MMP9, MMP14.<sup>9</sup>

It is postulated that inhibition of MMP13 will give rise to beneficial clinical effects in OA by blocking the destruction of cartilage, preventing deterioration of joint integrity and improving joint mobility.

The objective of the following medicinal chemistry programme was to identify orally active inhibitors of MMP13 for the treatment of OA. The candidate drug target profile called for a compound with potency/DMPK to support once a day oral dosing in man and also be structurally different from reverse hydroxamate and hydroxamic acid based MMP13 inhibitors.<sup>5,10–12</sup>

Reverse hydroxamate and hydroxamic acid based MMP13 inhibitors have been widely reported in the literature.<sup>12</sup> Previous reverse hydroxamate inhibitors **1a** and **2** from AstraZeneca have shown potent inhibition of cytochrome P450 isoform 3A4 (Cyp3A4)<sup>13,14</sup> and also time dependent inhibition (Fig. 1).<sup>15</sup> We have previously reported that the addition of a methyl group adjacent to the reverse hydroxamate moiety **1b** has been a successful strategy to reduce Cyp3A4 activity for aggrecanase inhibitors.<sup>13,14</sup> Unfortunately, this change also led to significant drops in MMP13 potency for these inhibitors.

Alternative zinc binding groups to the reverse hydroxamate, such as hydantoin (**3a**), have been used in-house to deliver potent MMP12 compounds for the treatment of COPD with significantly reduced Cyp3A4 liability.<sup>16</sup> Hydantoin **3a** had an attractive in vitro profile: moderate MMP13 potency (IC<sub>50</sub> 21 nM), clean cytochrome P450 isoform profile (>40 μM in 3A4, 2D6, 1A2, 2C9 and 2C19 isoforms), moderate solubility (23 μM) and stability in liver microsomes (Cl<sub>int</sub> <10 μL/min/mg in human, rat and dog).

\* Corresponding author. Tel.: +1 781 839 4682.

E-mail address: [chris.desavi2@astrazeneca.com](mailto:chris.desavi2@astrazeneca.com) (C. De Savi).

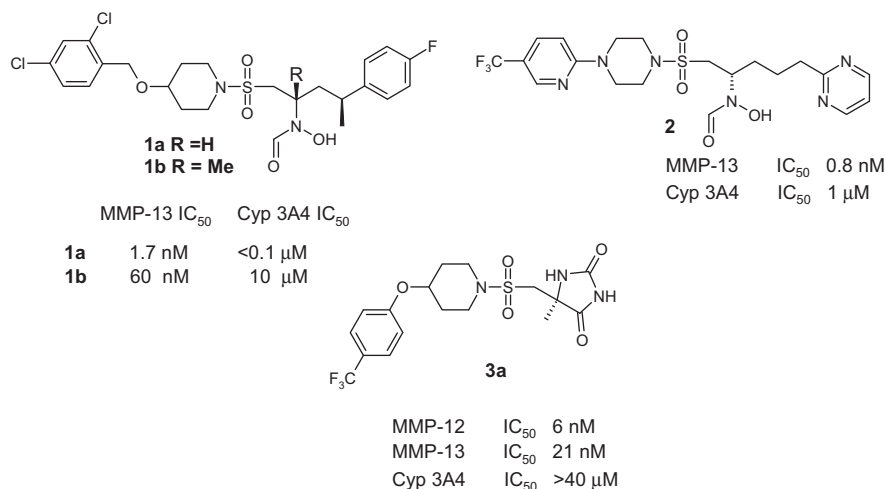


**Figure 1.** Historical AstraZeneca MMP13 and MMP12 compounds.

We chose to use the MMP12 compound as a start point and modify the pendant aryl ether to optimize MMP13 potency and other properties including aqueous solubility and MMP14 selectivity<sup>9</sup> (Table 1).

Previous SAR and X-ray structural information from the reverse hydroxamate series<sup>13,14</sup> showed that *ortho* substitution on the terminal aryl group was not tolerated and led to significant reductions in MMP13 potency; the 2,4-dichloro phenyl ether **3c** is 600× less potent compared to 4-Cl phenyl ether **3b** (7 μM and 12 nM, respectively). Similarly, *meta* substitution also resulted in a significant reduction in MMP13 potency (**3i** vs **3h**, 1.6 μM and 8.5 nM). Due to the good potency associated with *para*-ethyl ether **3e**, a wide variety of alkyl substituted ethers were prepared. A modest increase in MMP13 potency was achieved when replacing OEt with OCH<sub>2</sub>CF<sub>3</sub> but with no significant change in MMP14 selectivity.

Interestingly, the fully fluorinated matched pair compound **3n** maintained good MMP13 potency but led to significant increases in MMP14 selectivity (>1000×). The tetrafluorinated ether **3l** gave a balance of both excellent MMP13 potency and good MMP14 selectivity (550×) and reinforced the importance of fluoro substitution to MMP13 potency. The corresponding des-fluorinated matched pair compound **3o** was 60-fold less potent (LLE 7.1 vs 5.4). Replacing OEt (**3e**) with CH<sub>2</sub>OMe (**3p**) led to reductions in MMP13 potency. A wide variety of substituted benzyl and heterocyclic ethers were also prepared to explore MMP13 SAR, MMP14 selectivity and solubility (Table 2). Although substituted benzyl ethers gave excellent MMP13 potency (**4a–4g**), this change also resulted in poor solubility. F-benzyl ether **4f** had superior MMP14 selectivity (>2000×) compared to all other benzyl ethers tested. *Meta*-substituted CN derivative **4d** maintained very good MMP13

**Table 1**  
MMP13, MMP12, MMP14 potency and solubility data of piperidine ethers **3a–r**

Compd	R <sup>a</sup>	MMP-13 IC <sub>50</sub> <sup>b</sup> (nM)	MMP-12 IC <sub>50</sub> <sup>b</sup> (nM)	MMP-14 IC <sub>50</sub> <sup>b</sup> (nM)	cLogP	LLE <sup>c</sup>	Sol <sup>d</sup> (μM)
<b>3a</b>	CF <sub>3</sub>	21	5.9		1.8	5.9	23
<b>3b</b>	Cl	11.5	8.9		1.5	6.5	12
<b>3c</b>	2,4-Di-Cl	6980			1.8	3.4	
<b>3d</b>	F	28.9	23.7		0.9	6.6	52
<b>3e</b>	OEt	18.2	2	2817	1.3	6.5	15
<b>3f</b>	OCF <sub>3</sub>	59.1	3.3	9501	1.8	5.4	18
<b>3g</b>	OSO <sub>2</sub> Me	53.8			0.07	7.2	
<b>3h</b>	OCH <sub>2</sub> CF <sub>3</sub>	8.5		1950	1.5	6.6	34
<b>3i</b>	3-OCH <sub>2</sub> CF <sub>3</sub>	1617			1.5	4.3	
<b>3j</b>	OCH <sub>2</sub> CH <sub>2</sub> CF <sub>3</sub>	5.4		3121	1.5	6.8	110
<b>3k</b>	OCH <sub>2</sub> CF <sub>2</sub> CF <sub>3</sub>	2.6		4735	2.5	6.1	4.4
<b>3l</b>	OCH <sub>2</sub> CF <sub>2</sub> CHF <sub>2</sub>	1.2		553	1.8	7.1	32
<b>3m</b>	OCF <sub>2</sub> CHF <sub>2</sub>	4.7		2220	2.6	5.7	6.8
<b>3n</b>	OCF <sub>2</sub> CF <sub>3</sub>	9.8		>10,000	2.5	5.6	<2
<b>3o</b>	On-Pr	71.2		>10,000	1.8	5.4	
<b>3p</b>	CH <sub>2</sub> OMe	178			0.43	6.3	
<b>3q</b>	CH <sub>2</sub> SO <sub>2</sub> Me	1051			−1.2	7.2	
<b>3r</b>	CH <sub>2</sub> –4-pyridyl	8445			1.5	6.2	

<sup>a</sup> All substituents are *para*-substituted (4-position) unless otherwise indicated.

<sup>b</sup> For general assay procedures see Ref. 13; values mean of *n* = 2 experiments.

<sup>c</sup> LLE (Lipophilic Ligand Efficiency)<sup>17</sup> values are calculated as pIC<sub>50</sub>–clogP.

<sup>d</sup> Thermodynamic solubility (μM) in 0.1 M phosphate buffer pH 7.4 at constant temperature (25 °C) for 24 h.

potency but additionally had improved MMP14 selectivity compared to *para* CN benzyl ether **4c**. Methyl sulfone **4b** had the highest LLE but the poorest MMP14 selectivity in this subset of compounds. Due to the overall poor solubility associated with the benzyl ethers, a variety of pyridyl and other heterocyclic compounds were made to see if improvements in solubility could be achieved whilst maintaining target potency. The unsubstituted pyridyls (**4h–j**) were potent MMP13 inhibitors (high LLE) with incremental increases in MMP14 selectivity achieved as the nitrogen was moved from *para* to *meta* to *ortho* positions. Although the *clogP* of these compounds had decreased, only modest increases in solubility were achieved relative to the phenyl analogs.

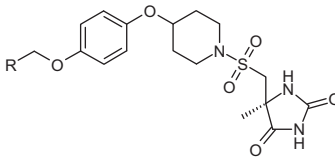
Nonetheless, 2-pyridyl **4j** had a good overall profile; excellent MMP14 selectivity ( $\sim 1500\times$ ) with acceptable solubility (20  $\mu\text{M}$ ) and no inhibition of cytochrome P450 ( $\text{IC}_{50} > 10 \mu\text{M}$ ; 3A4, 2D6, 1A2, 2C9 and 2C19 isoforms). The pharmacokinetic profiles in rat and dog showed low to moderate clearance ( $\text{Cl}_p = 17$  and 3 mL/min/kg, respectively) and good half lives ( $t_{1/2} = 2.5$  and 2.3 h, respectively) given the low volume of distribution ( $V_{\text{dss}} = 0.8$  and 0.6 L/kg). Oral bioavailability was moderate to good in rat and dog ( $F\% = 35$  and 51, respectively).

Heterocycles **4k** and **4l** maintained good MMP13 potency and good LLE, however thiadiazole **4l** showed reduced MMP14 selectivity. Trifluoromethyl substituted furan **4m** displayed excellent MMP13 potency and superior MMP14 selectivity ( $\sim 2200\times$ ). The most lipophilic ligand efficient compounds were **4l**, **4b** and **4h** (LLE 8.1, 8.0 and 7.7, respectively).

A second hydantoin series, piperazine pyrimidine benzyl ethers **5**, was also investigated in the lead optimization campaign (Table 3). Due to the poor solubility associated with the piperidine ethers, design in this area focused primarily on low *clogP* heterocyclic analogues.

The primary advantage of this series was the excellent MMP14 selectivity: all the compounds tested showed at least  $>1000\times$  fold selectivity ratios (vs MMP13), with isoxazole **5k** being very selective over MMP14 (26,000 $\times$ ). The most potent piperazine pyrimidine heterocycles were **5j**, **5k**, **5l** and **5m**, all showing sub 10 nM MMP13 potency and excellent MMP14 selectivity ratios. Isoxazole **5k** and thiazole **5m** were also the most ligand lipophilic efficient compounds (LLE 8.4 and 8.1, respectively). Pyrazole **5e** and imidazole **5f** were not potent MMP13 inhibitors, however rearranging the methyl substitution pattern from 1,5-dimethyl pyrazole (**5e**) to

**Table 2**  
MMP13, MMP12, MMP14 potency and solubility data of piperidine ethers **4a–m**



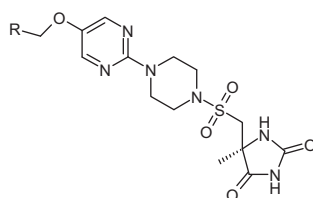
Compd	R	MMP-13 $\text{IC}_{50}^b$ (nM)	MMP-14 $\text{IC}_{50}^b$ (nM)	<i>cLogP</i>	LLE <sup>c</sup>	Sol ( $\mu\text{M}$ )
<b>4a</b>		1.4	671	2.5	6.4	<0.8
<b>4b</b>		1.4	62	0.85	8.0	3.1
<b>4c</b>		0.69	116	1.9	7.2	1.8
<b>4d</b>		1.8	915	1.9	6.8	4.4
<b>4e</b>		2.7	1080	2.4	6.2	1.2
<b>4f</b>		3.6	7731	2.6	5.8	NV
<b>4g</b>		0.88	764	2.6	6.4	NV
<b>4h</b>		1.9	450	0.99	7.7	130
<b>4i</b>		2.9	1282	0.99	7.5	8.4
<b>4j</b>		4.7	6897	0.99	7.3	20
<b>4k</b>		5.3	4090	0.83	7.5	87
<b>4l</b>		1.6	350	0.73	8.1	28
<b>4m</b>		0.82	1858	2.6	6.5	

NV = no value.

<sup>b</sup> See footnotes from Table 1.

<sup>c</sup> See footnotes from Table 1.

**Table 3**  
MMP-13, MMP-14, solubility and selected in vitro/in vivo rat PK of aryl piperazine pyrimidine ethers **5a–m**



Compd	R	MMP-13 IC <sub>50</sub> <sup>a</sup> (nM)	MMP-14 IC <sub>50</sub> <sup>a</sup> (nM)	cLogP	LogD	Sol <sup>b</sup> (μM)	Human Cl <sub>int</sub> <sup>c</sup> (μL/ min/mg)	Rat Cl <sub>int</sub> <sup>d</sup> (μL/min/ 10 <sup>6</sup> cells)	Rat Cl <sup>e</sup> (mL/ min/kg)	t <sub>1/2</sub> (h)	F <sup>f</sup> (%)
<b>5a</b>		14.0	>99,999	1.7	2.1	16	16	nt	4.8	1.9	nt
<b>5b</b>		3.3	53,584	0.9	1.6	66	<2	6.7	18.1	7.5	51
<b>5c</b>		13.8	>10,000	-0.1	1.1	1	nv				
<b>5d</b>		544.6		-0.9		560					
<b>5e</b>		1080		-0.1							
<b>5f</b>		73297329		-0.6							
<b>5g</b>		47.3		-0.1	0.8	32					
<b>5h</b>		31.5		-0.2	<0.5	49					
<b>5i</b>		17.7	>100,000	-0.2	0.7	13	<2	2.8	13.4	0.67	37
<b>5j</b>		2.8	>10,000	0.6	1.9	3.1	nt	nt	9.4	3.3	nt
<b>5k</b>		3.8	98,907	0.3			<2	<2			
<b>5l</b>		5.1	33,882	1.6	2.3	11	7.3	3.6	6.3	2.6	100
<b>5m</b>		8.3	>10,000	-0.4	1.2	14	16	28	97.3	0.23	6

<sup>a</sup> IC<sub>50</sub>'s were derived from triplicate measurements whose standard errors were normally <5% in a given assay. Assay to assay variability was within twofold based on the results of a standard compound; nt = not tested.

<sup>b</sup> Thermodynamic solubility (μM) in 0.1 M phosphate buffer pH 7.4 at constant temperature (25 °C) for 24 h.

<sup>c</sup> Human microsome metabolism intrinsic clearance Cl<sub>int</sub> (μL/min/mg). Cl<sub>int</sub> reported is mean of three separate experiments; nv = no value.

<sup>d</sup> For procedure see Ref. 18 Cl<sub>int</sub> reported is mean of three separate experiments.

<sup>e</sup> Compounds dosed at 2 mg/kg iv, n = 2 animals.

<sup>f</sup> Compounds dosed at 3–10 mg/kg p.o., n = 4 animals.

1,3-dimethyl pyrazole (**5g**) resulted in a significant increase in MMP13 potency (1080 nM and 47 nM, respectively).

The aryl piperazine hydantoin were relatively stable in both human microsomes and rat hepatocytes and a selected number of examples (**5a**, **5b**, **5i**, **5j**, **5l** and **5m**) were dosed in vivo to rat. These selected compounds all showed low to moderate clearance with V<sub>dss</sub> generally within the range of 0.5–2 L/kg leading to moderate iv half-lives, albeit thiazole **5m** was highly cleared in rat which led to poor bioavailability. Compounds **5b** and **5l** showed particularly acceptable t<sub>1/2</sub> (7.5 and 2.6 h, respectively) which warranted both oral profiling and further investigation in other species. *Meta* cyano benzyl hydantoin **5b** showed further good pharmacokinetic properties in both mouse and dog showing mod-

erate clearance with relatively high volumes leading to prolonged elimination half-lives (t<sub>1/2</sub> = 5.8, 7.5 and 5.4 h in mouse, rat and dog, respectively) coupled with excellent oral absorption in all pre-clinical species dosed (F% 50–100).

The single X-ray crystal structure of compound **5b** in MMP13 overlaid with a historical reverse hydroxamate **6** clearly shows the transposition of both the sulfonamide and pyrimidine motifs of the molecules (Fig. 2).<sup>19</sup> Both compounds are able to form H-bonds between the sulfonamide oxygens and backbone residues Leu185 and Ala186. The CN benzyl motif extends further into the MMP13 S1' pocket versus the trifluoroethyl ether. Both zinc binding groups also overlay well, however the *N*-hydroxyformamide group of **6** chelates Zn<sup>2+</sup> in a bidentate manner whereas the

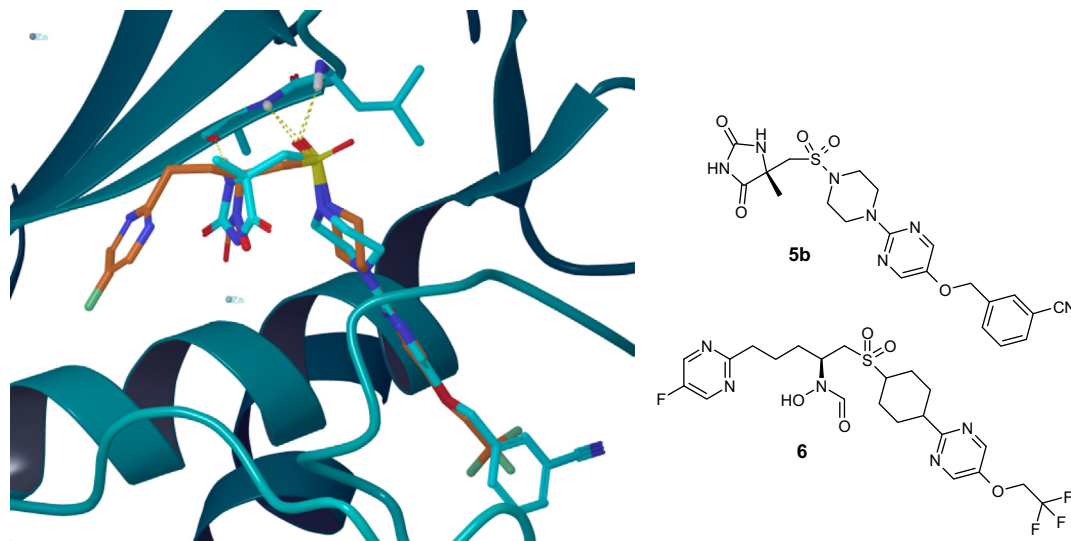


**Figure 2.** Overlay of bound compounds hydantoin **5b** (cyan) and representative reverse hydroxamate **6** (orange) from MMP13 crystal structure complexes. Key hydrogen bond interactions with active site residues of MMP13 are highlighted in yellow. The catalytic zinc ion (blue) is shown as a sphere.

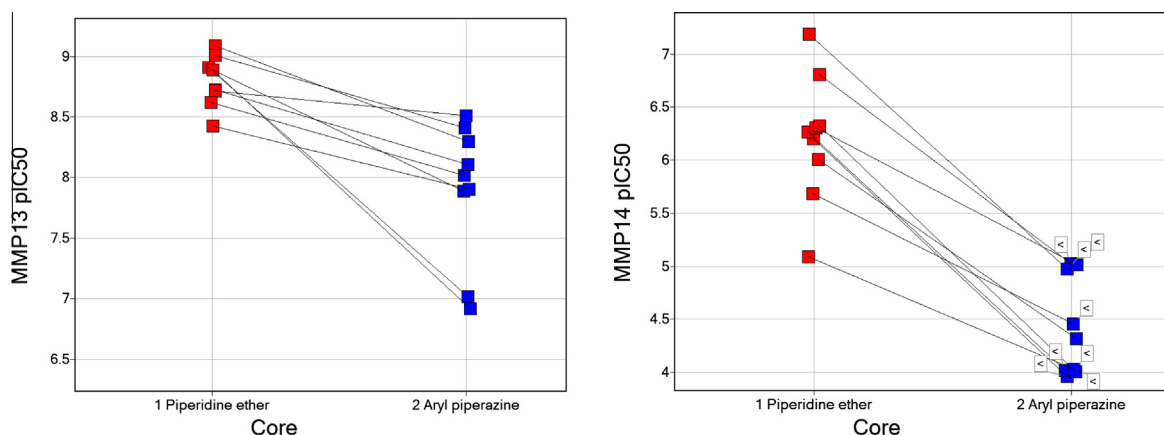


**Figure 3.** (a) MMP13 pIC<sub>50</sub> versus core substructure (red—piperidine benzyl ethers **4**; blue—aryl piperazine benzyl ethers **5**); lines attaching direct matched pairs. (b) MMP14 pIC<sub>50</sub> versus core substructure (<indicate 'less than' out of range measurements in MMP14 pIC<sub>50</sub> biochemical assay).

hydantoin **5b** forms a monodentate coordination with the Zn<sup>2+</sup> ion through the acidic N, with the additional NH forming a H-bond with the carbonyl of Ala186.

A number of benzyl ethers used in the piperazine pyrimidines **5** had been previously used in the piperidine benzyl ethers **4**, enabling a Matched Molecular Pair Analysis.<sup>20</sup> On average, the MMP-13 potency of the piperazine pyrimidine benzyl ethers **5** was reduced by approximately 0.5 log unit compared to their piperidine ether analogues (Fig. 3a, mean difference in MMP13 pIC<sub>50</sub> = 0.9, standard error of mean = 0.20, *N* = 9 pairs). Nonetheless the aryl piperazines were significantly more selective versus MMP14 (Fig. 3b, mean difference in MMP14 pIC<sub>50</sub> >1.8, standard error of mean = 0.25, *N* = 9 pairs), presumably due to the benzyl ether extending deeper into the MMP13 S1' pocket and causing negative interactions with the shorter MMP14 S1' pocket.<sup>21</sup>

Due to the excellent MMP13 potency, acceptable cross-MMP selectivity profile and in vitro stability observed in both human microsomes and hepatocytes, compounds **3m** and **5l** were selected for further advanced in vivo profiling (Table 4). Piperidine **3m** is a potent inhibitor of MMP13 (IC<sub>50</sub> 4.7 nM). It exhibits a 25- to 100-fold selectivity against MMP3, 8 and 15; 150 to 550-fold selectivity against MMP16, 14, 19 and ADAM-17; and >2000-fold selectivity against MMP1, 7, ADAM-9, ADAM-10 and ADAM-TS4.<sup>13,14</sup> Further-

more, it has good physicochemical properties and excellent ADME parameters. **3m** has very low in vivo clearance in both rat and dog (0.4 and 0.2 mL/min/kg, respectively) and shows no turnover in either human microsomes or hepatocytes (additionally no turnover is seen in dog hepatocytes). The predicted dose to man (pred. DTM) assuming that free blood levels at C<sub>min</sub> equal to 3 × MMP13 IC<sub>50</sub> is 0.04 mg/kg/day based on a predicted human clearance 0.07 mL/min/kg, *V*<sub>dss</sub> 0.76 L/kg (both estimated using rat/dog allometry) and *F*<sub>u</sub> 0.05.<sup>22</sup> PB-PK modelling gives a pred. DTM 0.06 mg/kg/day.<sup>23</sup> The low dose to man is primarily driven by a long predicted half-life in man (*t*<sub>1/2</sub> 122 h). In contrast, furan **5l** has a higher pDTM 0.54 mg/kg/day based on a predicted human clearance of 0.7 mL/min/kg, *V*<sub>dss</sub> 0.9 L/kg, *F*<sub>u</sub> 0.04 and a shorter predicted half-life in man (*t*<sub>1/2</sub> 16 h). Furan **5l** has a significantly improved MMP14 selectivity profile. Neither compound inhibits the five most common human cytochrome P450 isoforms at 10 μM or below, nor is there time dependent inhibition of human P450 3A4 at 50 μM.

The synthesis of compound **3m** is concisely described in Scheme 1.<sup>27,28</sup> Tetrafluoroethoxy phenol **9** was prepared in high yield from the commercially available bromide **8** via a lithium halogen exchange reaction followed by quenching the intermediate boronate ester with H<sub>2</sub>O<sub>2</sub>. The resultant phenol was subjected

**Table 4**  
Profiles of advanced compounds **3m** and **5l**<sup>28</sup>

Parameter	<b>3m</b>	<b>5l</b>
MMP13 IC <sub>50</sub> <sup>a</sup>	4.7 nM	5.1 nM
MMP 14 selectivity <sup>a</sup>	430	14871
MMP 1/2/3/8/19 selectivity <sup>a</sup>	>1989/0.6/60/50/547	>1809/32/47/180/7
Log D <sub>7.4</sub>	2	2.3
FASIF solubility <sup>b</sup> (μM)	14.9	26.5
Dose solubility <sup>25</sup> (q.d./b.i.d.)	389/194	2545/1018
Hu/rat/dog %free	5/3/5	6/8/8
Hu Mics <sup>c</sup> /Heps Cl <sub>int</sub> <sup>d</sup>	<2/<2	7/<2
Cyp Inhib IC <sub>50</sub> <sup>e</sup>	>10 μM (5/5)	>10 μM (5/5)
hERG IC <sub>50</sub> <sup>26</sup>	40 μM	44 μM
Caco-2 (@10 μM) <sup>f</sup>	21 × 10 <sup>-6</sup> AB/52 × 10 <sup>-6</sup> BA	9 × 10 <sup>-6</sup> AB/52 × 10 <sup>-6</sup> BA
Rat PK <sup>g</sup> Cl/ t <sub>1/2</sub> /V <sub>dss</sub>	0.4 mL/min/kg/16 h/0.6 L/kg	6.3 mL/min/kg/2.6 h/1.3 L/kg
Dog PK <sup>h</sup> Cl/t <sub>1/2</sub> /V <sub>dss</sub>	0.2 mL/min/kg/35 h/0.6 L/kg	1.3 mL/min/kg/10.6 h/1.2 L/kg
Rat/Dog/F%	64/40	100/51
Human pred. PK Cl/t <sub>1/2</sub> /V <sub>dss</sub>	0.07 mL/min/kg/122 h/0.76 L/kg	0.7 mL/min/kg/16 h/0.9 L/kg
Human pred. DTM Dose (mg/day)	2.8 q.d.	38 q.d.
Human pred. Free C <sub>max</sub> (μM)	0.37	0.34

<sup>a</sup> For general assay procedures see Ref. 13 IC<sub>50</sub> values were derived from at least six measurements whose standard errors were normally <5% in a given assay. Assay to assay variability was within twofold based on the results of a standard compound.

<sup>b</sup> FASIF—Fasted simulated intestinal fluid solubility (μM). See Ref. 24

<sup>c</sup> Human microsome metabolism intrinsic clearance Cl<sub>int</sub> (μL/min/mg microsomal protein). Cl<sub>int</sub> reported is mean of six separate experiments.

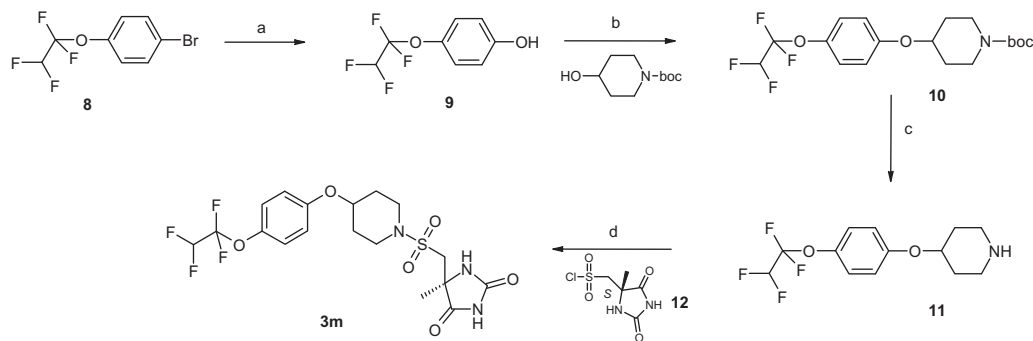
<sup>d</sup> Human hepatocyte metabolism intrinsic clearance Cl<sub>int</sub> (μL/min/10<sup>6</sup> cells). Cl<sub>int</sub> reported is mean of six separate experiments.

<sup>e</sup> Inhibition of cytochrome P450 isoforms: 1A2, 2C9, 2C19, 2D6 and 3A4.

<sup>f</sup> Apparent permeability (P<sub>app</sub> cm/s × 10<sup>-6</sup>) in human colon carcinoma (Caco-2) cells at 10 μM/pH7.4. AB—apical to basolateral direction; BA—basolateral to apical direction (efflux).

<sup>g</sup> Compounds dosed at 2 mg/kg iv, n = 2 animals and 5 mg/kg p.o., n = 4 animals.

<sup>h</sup> Compounds dosed at 0.5 mg/kg iv, n = 4 animals and 1 mg/kg p.o., n = 4 animals.



**Scheme 1.** Reagents and conditions: (a) *n*-Buli and triisopropyl borate, −50 to −20 °C then H<sub>2</sub>O<sub>2</sub>, 85%; (b) triphenylphosphine, DTAD, DCM, 64%; (c) 4 M HCl, dioxane, 70%; (d) DIPEA, THF, −10 °C to rt, 51%.

to a Mitsunobu reaction with commercially available *N*-Boc piperidinol to deliver compound **10** which was then deprotected with HCl to deliver piperidine **11** in quantitative yield. The coupling of chirally pure sulfonyl chloride hydantoin **12**<sup>28</sup> and piperidine **11** in the presence of DIPEA successfully furnished compound **3m** in 51% yield after chromatography as a white solid.

The effect of compound **3m** on cartilage loss was evaluated by magnetic resonance imaging (MRI) in the Dunkin Hartley guinea pig model of spontaneous osteoarthritis.<sup>29</sup> The guinea pig spontaneous model of osteoarthritis is considered to mimic aspects of articular cartilage degradation in humans.<sup>30</sup> Briefly, guinea pigs knee were imaged in vivo by high-resolution three-dimensional (3D) MRI at 9 months of age. Animals were randomised into either

vehicle (20% DMSO, 80% PEG, n = 6), compound **3m** (11 mg/kg/day, n = 7), or the MMP13 reference compound<sup>31</sup> (0.06 mg/kg/day in 20% DMSO, 60% PEG, 20% water, n = 6) previously shown to be efficacious in this study. Compounds were administered continuously by subcutaneous osmotic mini-pump implanted 7 days post initial MRI imaging. A second MRI image was obtained approximately 12 weeks later and image analysis performed to assess quantitative volumetric changes of the medial tibial cartilage. PK analysis confirmed that **3m** reached sufficient exposure to provide free cover over guinea pig MMP13 between 1- and 5.6-fold IC<sub>50</sub>, respectively, at termination. MRI results, shown in Figure 4 demonstrate vehicle treated animals lost ~23% medial tibial cartilage volume. In contrast, both reference compound<sup>31</sup> and **3m** treatment resulted in



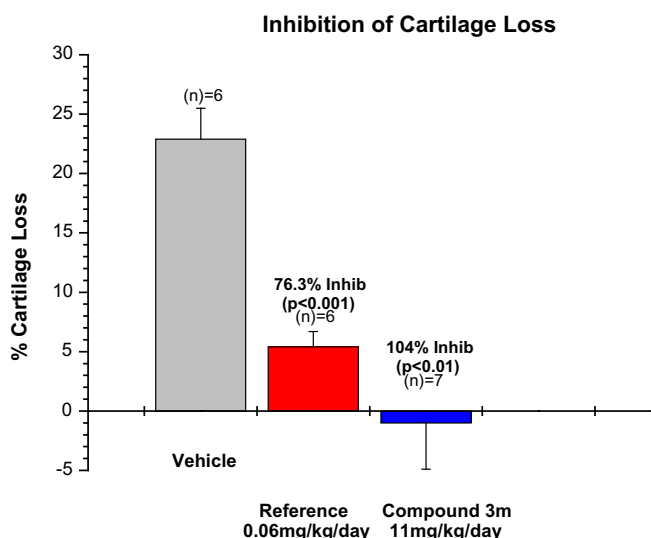


**Figure 4.** % Cartilage loss versus compound: Effect of compound **3m** (and MMP13 reference compound<sup>31</sup>) on MRI assessed medial tibial cartilage volume loss in the guinea pig model of spontaneous OA.

a statistically significant inhibition of cartilage loss (76% and 104%, respectively).

Compound **3m** is free of hERG activity up to 50  $\mu$ M (hERG index ~2778) and was found not to be mutagenic in SOS/umu, Ames and mouse lymphoma screens. Furthermore, no significant activities were detected at ~100 $\times$  free  $C_{max}$  against 141 additional targets (unrelated proteases, ion channels, receptors and transporters) in wider secondary pharmacology screening. Due to the potent in vivo activity and benign in vitro safety profile, **3m** was advanced into rat 28 day toxicity studies. In rat, there were no mortalities, significant clinical observations, effects on body weight, food and water consumption, or significant changes in clinical chemistry or hematological parameters. Interestingly, it did not cause any changes to the connective tissue, including fibrodysplasia (the expected significant change) in this study.

In summary, this lead optimization program delivered several high quality hydantoin which showed potent MMP13 potency, good MMP14 selectivity, low in vitro human  $Cl_{int}$ , which when coupled with low pre-clinical in vivo clearance, confidently suggests low in vivo human clearance. There is also no cytochrome P450 or time dependent inhibition commonly associated with the historical reverse hydroxamate series. Several strategies were employed to deliver compounds with acceptable overall solubility profiles without compromising excellent DMPK properties and ultimately leading to advanced candidates supporting once-a-day oral dosing regimens in man.

In conclusion, several novel series of MMP13 hydantoin inhibitors were discovered by replacing the zinc binding reverse hydroxamate with a hydantoin group. Lead optimisation from an MMP12 hydantoin hit was undertaken via a variety of modifications made to the P1' group leading to three discrete hydantoin sub-series. Compound **3m** was progressed into development for the treatment of osteoarthritis by AstraZeneca as AZD6605.<sup>32</sup>

## Acknowledgments

We would like to thank Liz Flavell who produced the MMP13 protein, David Hargreaves for crystallization and depositing structures into RCSB protein data bank, Stefan Gerhardt for crystallography determination and Attila Ting for modeling structures and general suggestions for the paper. And final thanks to both John

G. Cumming and David A. Scott for technical suggestions and proof-reading the manuscript.

## Supplementary data

Supplementary data (experimental procedures and characterisation data for compounds **3m**, **5b** and **5l**) associated with this article can be found, in the online version, at <http://dx.doi.org/10.1016/j.bmcl.2013.05.089>.

## References and notes

- Altman, R.; Asch, E.; Bloch, D.; Bole, D.; Borenstein, K.; Brandt, W.; Christy, W.; Cooke, T. D.; Greenwald, R.; Hochberg, M.; Howell, D.; Kaplan, D.; Koopman, W.; Longley, S.; Mankin, H.; McShane, D. J.; Medsger, T.; Meenan, R.; Mikkelsen, W.; Moskowitz, R.; Murphy, W.; Rothschild, B.; Segal, M.; Sokoloff, L.; Wolfe, F. *Arthritis Rheum.* **1986**, *29*, 1039.
- Helmick, C. G.; Felson, D. T.; Lawrence, R. C.; Gabriel, S.; Hirsch, R.; KentKwoh, C.; Liang, M. H.; MaraditKremers, H.; Mayes, M. D.; Merkel, P. A.; Pillemer, S. R.; Reveille, J. D.; Stone, J. H. *Arthritis Rheum.* **2008**, *58*, 15.
- Symmons, D. P.; Mathers, C. D.; Pfleger, B. 'The Global Burden of Osteoarthritis in the Year 2000' GBD 2000 Working Paper, World Health Organisation, Geneva. [http://www.who.int/healthinfo/statistics/bod\\_osteoarthritis.pdf](http://www.who.int/healthinfo/statistics/bod_osteoarthritis.pdf). Accessed March 2013.
- Conaghan, P.; Birrell, F.; Burke, M.; Cumming, J.; Dickson, J.; Dieppe, P.; Doherty, M.; Dziedzic, K.; Francis, R.; Grant, R.; Kell, C.; Latimer, N.; MacGregor, A.; Naisby, C.; O'Mahony, R.; Oliver, S.; Richards, A.; Underwood, M. *Osteoarthritis: National Clinical Guideline for Care and Management in Adults*; NICE, Royal College of Physicians: London, 2008.
- Hu, J.; Van den Steen, P. E.; Sang, Q.-X. A.; Opdenakker, G. *Nat. Rev. Drug Disc.* **2007**, *6*, 480.
- Mitchell, P. G.; Magna, H. A.; Reeves, L. M.; Lopresti-Morrow, L. L.; Yocum, S. A.; Rosner, P. J.; Geoghegan, K. F.; Hambor, J. E. *J. Clin. Invest.* **1996**, *97*, 761.
- Bigg, H. F.; Rowan, A. D. *Curr. Opin. Pharmacol.* **2001**, *1*, 314.
- Brown, P. D. *Expert Opin. Investig. Drug* **2000**, *9*, 2167.
- Peterson, T. *Cardiovasc. Res.* **2006**, *69*, 677.
- Whittaker, M.; Floyd, C. D.; Brown, P.; Gearing, A. J. H. *Chem. Rev.* **1999**, *99*, 2735.
- Jacobsen, J. A.; Major Jourden, J. L.; Miller, M. T.; Cohen, S. M. *Biochim. Biophys. Acta* **2010**, *1803*, 72.
- Li, N.-G.; Shi, Z.-H.; Tang, Y.-P.; Wang, Z.-J.; Song, S.-L.; Qian, L.-H.; Qian, D.-W.; Duan, J.-A. *Curr. Med. Chem.* **2011**, *18*, 977.
- De Savi, C.; Pape, A.; Cumming, J. G.; Ting, A.; Smith, P. D.; Burrows, J. N.; Mills, M.; Davies, C.; Lamont, S.; Milne, D.; Cook, C.; Moore, P.; Sawyer, Y.; Gerhardt, S. *Bioorg. Med. Chem. Lett.* **2011**, *21*, 1376.
- De Savi, C.; Pape, A.; Cumming, J. G.; Ting, A.; Smith, P. D.; Tart, J.; Page, K.; Davies, C.; Lamont, S.; Milne, D.; Moore, P.; Sawyer, Y. *Bioorg. Med. Chem. Lett.* **2011**, *21*, 3301.
- Riley, R.; Grime, K.; Weaver, R. *Expert Opin. Drug Metab. Toxicol.* **2007**, *3*, 51.
- (a) Eriksson, A.; Lepisto, M.; Lundkvist, M.; Munck Af Rosenschold, M.; Zlatoidsky, P. WO 02/074767, 2002; *Chem. Abstr.* **2002**, *137*, 263031.; (b) Eriksson, A.; Lepisto, M.; Lundkvist, M.; Munck Af Rosenschold, M.; Zlatoidsky, P. WO 02/074750, 2002; *Chem. Abstr.* **2002**, *137*, 247696.
- Leeson, P. D.; Springthorpe, B. *Nat. Rev. Drug Disc.* **2007**, *6*, 881.
- Houston, J. B.; Carlile, D. J. *Drug Metab. Rev.* **1997**, *29*, 891.
- The X-ray crystal ligand-protein structures of both compounds **5b** (PDB ID = 4JPA) and **6** (PDB ID = 4JP4) have been deposited into the RCSB Protein data bank (<http://www.pdb.org/pdb/home/home.do>).
- Leach, A. G.; Jones, H. D.; Cosgrove, D. A.; Kenny, P. W.; Ruston, L.; MacFaul, P.; Wood, J. M.; Colclough, N.; Law, B. J. *Med. Chem.* **2006**, *49*, 6672.
- (a) De Savi, C.; Morley, A. D.; Ting, A.; Nash, I.; Karabelas, K.; Wood, C. M.; James, M.; Norris, S. J.; Karoutchi, G.; Rankine, N.; Hamlin, G.; MacFaul, P. A.; Ryan, D.; Baker, S. V.; Hargreaves, D.; Gerhardt, S. *Bioorg. Med. Chem. Lett.* **2011**, *21*, 4215.; (b) De Savi, C.; Morley, A. D.; Ting, A.; Nash, I.; Karoutchi, G.; Page, K.; Gerhardt, S. *Bioorg. Med. Chem. Lett.* **2011**, *22*, 271.
- McGinnity, D.; Collington, J.; Austin, R.; Riley, R. *Curr. Drug Metab.* **2007**, *8*, 463.
- Willmann, S.; Schmitt, W.; Keldenich, J.; Lippert, J.; Dressman, J. B. *J. Med. Chem.* **2004**, *47*, 4022.
- (a) Galia, E.; Nicolaides, E.; Hörter, D.; Löbenberg, R.; Reppas, C.; Dressman, J. B. *Pharm. Res.* **1998**, *15*, 698.; (b) Dressman, J. B.; Amidon, G. L.; Reppas, C.; Shah, V. P. *Pharm. Res.* **1998**, *15*, 11.; (c) Dressman, J. B.; Reppas, C. *Eur. J. Pharm. Sci.* **2000**, *11*, 573.
- Rinaki, E.; Valsami, G.; Macheras, P. *Pharm. Res.* **1917**, *2003*, 20.
- Bridgland-Taylor, M. H.; Hargreaves, A. C.; Easter, A.; Orme, A.; Harmer, A.; Henthorn, D. C.; Ding, M.; Davis, A.; Small, B. G.; Heapy, C. G.; Abi-Gerges, N.; Paulsson, F.; Jacobson, I.; Schroeder, K.; Neagle, B.; Albertson, N.; Hammond, T. G.; Sullivan, M.; Sullivan, E.; Valentin, J.-P.; Pollard, C. E. *J. Pharmacol. Toxicol. Methods* **2006**, *54*, 189.
- Full experimental for the preparation and analytical data of compounds **3m**, **5b** and **5l** can be found in Supplementary data.
- Waterson, D.; Persson, D. J. WO 06/064218, 2006; *Chem. Abstr.* **2006**, *145*, 83331.

29. Tessier, J. J.; Bowyer, J.; Brownrigg, N. J.; Peers, I. S.; Checkley, D. R.; Westwood, R. F.; Waterton, J. C.; Maciewicz, R. A. *Osteoarthritis Cartilage* **2003**, *11*, 845.
30. Bendele, A. M.; Hulman, J. F. *Arthritis Rheum.* **1988**, *31*, 561.
31. MMP13 historical internal reference compound: *N*-hydroxy-*N*-[(1*S*)-3-(2-pyrimidinyl)-1-[[[4-[5-(2,2,2-trifluoroethoxy)-2-pyridinyl]-1-piperazinyl]sulfonyl]methyl]propyl]-formamide).
32. AZD6605 was made available free of charge to UK medical researchers in a recent agreement between the Medical Research Council (MRC) and AstraZeneca, <http://www.pharmatopics.com/2011/12/astrazeneca-grants-uk-academia-free-access-to-its-patented-compounds/>. Accessed March 2013.